Polyhedron 160 (2019) 157–162

Contents lists available at ScienceDirect

Polyhedron

journal homepage: www.elsevier.com/locate/poly

Phenyl substituted ditelluro-imidodiphosphinate complexes of iron, nickel, palladium and platinum, and their pyrolysis studies generating metal tellurides

Temidayo Oyetunde [a,b], Mohammad Afzaal [c,*], Paul O'Brien [b,1]

[a] Centre for Chemical and Biochemical Research (CCBR), Redeemer's University, Ede, P.M.B. 230, Osun State 232102. Nigeria
[b] School of Chemistry and School of Materials, The University of Manchester, Oxford Road, Manchester M13 9PL, United Kingdom
[c] Maths and Natural Sciences Division, Higher Colleges of Technology, P.O. Box: 7947, Sharjah, United Arab Emirates

ARTICLE INFO

Article history:
Received 13 November 2018
Accepted 14 December 2018
Available online 28 December 2018

Keywords:
Single-source precursors
Metal tellurides
Antiferromagnetic
Imidodiphosphinate ligands
X-ray photoelectron spectroscopy

ABSTRACT

The tellurium complexes $M[N(PPh_2Te)_2]_n$ (M = Fe (**1**), Ni (**2**), Pd (**3**), Pt (**4**) and $n = 2$ or 3) have been prepared using the ditellurido anions $[N(PPh_2Te)_2]^-$ and their ability to generate tellurides was investigated by pyrolysis in a quartz glass tube, under vacuum at 500 °C for 90 min. The products were characterised by X-ray powder diffraction (XRD), scanning electron microscopy (SEM), energy dispersive analysis of X-rays (EDAX) and X-ray photoelectron spectroscopy (XPS). The XRD revealed an orthorhombic phase for the metal telluride from **1**, while the hexagonal phase was observed for tellurides from **2**, **3** and **4** respectively. Magnetic measurements on $FeTe_2$ (from **1**) indicated an antiferromagnetic sample with a transition temperature at 75 K.

1. Introduction

Dichalcogenoimidodiphosphinates, $[N(PR_2E)_2]^-$ (R = alkyl, aryl; E = S, Se) are chelating ligands that readily form cyclic complexes with main group, transition, lanthanides and actinides [1] metals. The useful synthesis of $[N(PPh_2Te)_2]^-$ was developed by Chivers et al. [2] using the anion $[N(PPh_2)_2]^-$. The sodium salts of the ditellurido ligands $[N(PR_2Te)_2]^-$ were obtained in good yields (R = ^{i}Pr, Ph, ^{t}Bu) [2,5,6]. Metal complexes of the ditellurido ligands $[N(PR_2Te)_2]^-$ have shown novel structures and new reaction chemistry in which the tellurium donor sites exhibit greater flexibility than sulfur or selenium, having a tellurium-centered ligand bridging two metal centres. Metal tellurides have potential applications as low band gap semiconductor materials in solar cells, thermoelectric devices and telecommunications. [3,4] This is because the peculiar and valuable properties of tellurium have resulted in its extensive research as an important p-type narrow band gap semiconductor. These properties include photoconductivity, piezoelectricity, thermoelectricity, non-linear optical responses and photoelectricity [7–9]. Metal complexes of the isopropyl derivative anion $[N(P^iPr_2Te)_2]^-$ have been shown to serve as efficient single-source precursors for pure metal telluride thin films or nanomaterials, e.g. CdTe, PbTe, In_2Te_3 [10–12].

Nickel telluride is an important intermetallic compound of the 3d transition metal chalcogenides series, for which various properties have been previously studied [13–16]. Some of these are electric, magnetic, crystallographic (helical chain conformation) and thermodynamic properties. The nickel-telluride system consists of two ordered compounds: NiTe and $NiTe_2$, with a range of continuous solid solutions between them [17]. Oftedal [18] reported that NiTe has a hexagonal structure of the NiAs-(B8)-type, while Tengnér [19] reported $NiTe_2$ to have the hexagonal $Cd(OH)_2$-(C6)-type structure. In a crystal of nickel telluride, the Ni^{2+} ions occupy a simple hexagonal lattice, while the Te^{2-} ions occupy a close-packed hexagonal lattice, with both lattices penetrating each other [13]. Also, NiTe can be used as an ohmic contacting layer of II–VI semiconductors because of their distinctive electrical transport property [16]. For reports on the deposition of nickel telluride, there are only a few, such as flash evaporation [20], AACVD [21] and electrodeposition [22].

The early synthesis of palladium ditelluride was reported by Thomassen [22] and Wöhler et al. [23] by preparing it as the only compound from the reaction of the constituent elements. Also, Groeneveld [24] prepared the compound by fusing the elements in the correct atomic proportions. Palladium monotelluride was also prepared by Thomassen by dry fusion of the elements in evacuated tubes [22]. About nine binary phases of the palladium-tellurium system are known, which include $Pd_{17}Te_4$, Pd_3Te, $Pd_{20}Te_7$, Pd_8Te_3, Pd_7Te_3, Pd_9Te_4, Pd_3Te_2, PdTe and $PdTe_2$ [25]. However, the most important of these seems to be PdTe

* Corresponding author.
E-mail address: mafzaal@hct.ac.ae (M. Afzaal).
[1] Deceased.

https://doi.org/10.1016/j.poly.2018.12.038
0277-5387/

and $PdTe_2$ because of their similar structural type with NiAs and CdI_2 respectively [24,25]. As a nanocrystal, palladium telluride can be applied as a catalyst for methanol electro-oxidation and it also behave as a strongly coupled superconductor [26]. The early synthesis of platinum telluride involved both wet and dry procedures as the main synthetic routes [24]. The wet method involved the reaction of hydrogen telluride with a solution of platinum metal salt, while the dry route was based on the direct fusion of the weighed constituents. In the platinum-tellurium system, the most important phases are PtTe and $PtTe_2$ [27]. According to Groeneveld [24], $PtTe_2$ has a CdI_2 structural type while PtTe consists of an orthorhombic structure [27].

$FeTe_2$ is an example of crystalline transition metal ditellurides in the 3d series known to exhibit 3D magnetic ordering and semiconductivity [28]. $FeTe_2$ is a marcasite, containing a narrow 3d band (about 1 eV), and is known to exhibit good magnetic properties [28], semiconductivity [29], high electrical conductivity [30] and high thermoelectric powder values [30]. Traditionally, $FeTe_2$ had been prepared by the direct contact of the elements in sealed tubes [31], while new synthetic routes involved OMVPE and MOCVD [32,33]. Through a solution-based solvothermal reduction, $FeTe_2$ nanoparticles were obtained [28,31]. From the precursor [Fe{$^tBu_2P(Te)NR$}$_2$] using gas-phase deposition, thin films of $FeTe_2$ were obtained by Song and Bochmann [34].

In this work, telluride complexes of iron (**1**), nickel (**2**), palladium (**3**) and platinum (**4**) have been prepared and characterized, using the phenyl substituted anionic $[N(PPh_2Te)_2]^-$ ligand. Samples were pyrolysed under vacuum in a quartz glass reactor. This yielded black deposits which were analysed by X-ray powder diffraction (XRD), scanning electron microscopy (SEM) and energy dispersive analysis of X-rays (EDAX) studies. Magnetic and conductivity measurements were attempted on various resulting materials to determine their properties.

2. Experimental

2.1. Materials and methods

All synthetic procedures were done under an inert atmosphere using a double manifold Schlenk-line, attached to an Edwards E2M8 vacuum pump and a dry nitrogen cylinder. Solid air-sensitive compounds were handled in a glove box under an inert atmosphere of dry nitrogen. Chemicals were purchased from Sigma-Aldrich and Fischer Chemicals and were used as received. Dry solvents were used throughout the syntheses, either distilled over standard drying agents (Na/benzophenone, CaH_2 etc.) or purchased and stored in flasks over molecular sieves. Elemental analyses were performed by the microanalysis section of the School of Chemistry, University of Manchester. TGA measurements were performed using a Seiko SSC5200/S220TG/DTA model with a heating rate of 10 °C min^{-1} under nitrogen. NMR spectra were recorded using a Bruker Avance (III) 400 MHz FT-NMR spectrometer, using $CDCl_3$ or d_8-toluene as the solvent. ^1H NMR spectra were referenced to the solvent signal and the chemical shifts were reported relative to Me_4Si. ^{31}P NMR spectra were referenced externally to an 85% solution of H_3PO_4 and the chemical shifts were reported relative to H_3PO_4. Conductivity studies on NiTe and PdTe involved wire connection to a Keithley 2400 source meter. Electricity of 0–2 V was applied and the I-V curve was obtained to determine the flow of current or otherwise.

2.2. Synthesis of $[NaN(PPh_2)_2]$ [2]

Toluene (75 ml) was added to a mixture of solid $[HN(PPh_2)_2]$ (13.30 g, 34.45 mmol) and NaH (0.84 g, 34.84 mmol). The amine TMEDA (10.40 ml, 69.09 mmol) was added to the suspension, which was heated to 100 °C for 6 h. The resulting suspension was allowed to settle and the yellow mother liquor decanted. The crude solid was suspended in hexane, washed with hexane (3 × 20 ml) and dried under vacuum to give a creamy white powder. Yield: 9.00 g, 65%.

2.3. Synthesis of (TMEDA)Na[$(TePPh_2)_2N$] [11]

Toluene (20 ml) was added to solid $[NaN(PPh_2)_2]$ (4.13 g, 10.14 mmol) and tellurium powder (2.64 g, 20.67 mmol). The ligand TMEDA (1.52 ml, 10.14 mmol) was added to the suspension, which was heated at 80 °C for 3 h. The resulting mixture was filtered at room temperature through a sintered glass to give a clear deep red solution. This was decanted and the residue washed with hexane (3 × 15 ml), followed by drying under vacuum to give a yellow polycrystalline powder. Yield: 2.00 g, 24%.

2.3.1. Synthesis of the complexes

All the complexes were prepared by modifying the procedures reported in the literature. Also, all attempts to grow quality crystals from solutions of these complexes were unsuccessful. Concentrated solutions of the complexes in THF layered with hexane at room temperature were prepared, but no growth was observed after several weeks. The reason(s) for this remained unclear.

2.4. Synthesis of [Fe{$(TePPh_2)_2N$}$_3$] (**1**)

A solution of (TMEDA)Na[$(TePPh_2)_2N$] (1.50 g, 1.86 mmol) in THF (25 ml) was added via cannula to a solution of $FeCl_3$ (0.10 g, 0.62 mmol) in THF (15 ml) at room temperature. The resulting brown solution was stirred for 2 h, followed by solvent removal under reduced pressure. Fresh THF (25 ml) was added, filtered and concentrated under vacuo. Hexane (25 ml) was added and the obtained solution was refrigerated overnight, followed by solvent removal under vacuum. A brown powder was obtained. Yield: 0.90 g, 74%. Elemental analysis calculated for $C_{72}H_{60}FeN_3P_6Te_6$: C, 43.77; H, 3.06; N, 2.13; P, 9.42%. Found: C, 45.80; H, 4.10; N, 2.84; P, 10.27%.

2.5. Synthesis of [Ni{$(TePPh_2)_2N$}$_2$] [35] (**2**)

A solution of (TMEDA)Na[$(TePPh_2)_2N$] (0.80 g, 0.992 mmol) in THF (20 ml) was added via cannula to a solution of $Ni(OAc)_2$ (0.12 g, 0.50 mmol) in THF (15 ml) at room temperature. A colour change from green to brown occurred and the solution was stirred for 2 h, followed by solvent removal under vacuo. Fresh THF (20 ml) was added and the solution filtered. Hexane (25 ml) was added and the resulting solution was left overnight, after which the solvent was removed to give a brown powder. Yield: 0.41 g, 65%. Elemental analysis calculated for $C_{48}H_{40}NiN_2P_4Te_4$: C, 43.07; H, 3.01; N, 2.09; P, 9.26%. Found: C, 45.25; H, 4.11; N, 2.64; P, 11.89%. ^1H NMR, (δ, ppm, $CDCl_3$, 400 MHz): 6.5–8.3 (m, Ar*H*); $^{31}P\{^1H\}$ NMR (δ, ppm, $CDCl_3$): 10.29.

2.6. Synthesis of [Pd{$(TePPh_2)_2N$}$_2$] [36] (**3**)

A solution of (TMEDA)Na[$(TePPh_2)_2N$] (0.80 g, 0.99 mmol) in THF (25 ml) was added via cannula to a solution of $Pd(OAc)_2$ (0.11 g, 0.50 mmol) in THF (20 ml) at room temperature. The resulting dark orange solution was stirred for 2 h, followed by solvent removal under reduced pressure. Fresh THF (25 ml) was added and the solution filtered. The clear filtrate was left overnight, giving an orange deposit from which solvent was removed to give a dark orange powder. Yield: 0.5 g, 74%. Elemental analysis calculated for $C_{48}H_{40}PdN_2P_4Te_4$: C, 41.59; H, 2.91; N, 2.02; P, 8.95%.

Found: C, 43.77; H, 3.08; N, 2.54; P, 10.34%. ^{1}H NMR (δ, ppm, $CDCl_3$, 400 MHz): 6.8–7.9 (m, Ar*H*); ^{31}P {^{1}H} NMR (δ, ppm, $CDCl_3$): 22.4.

2.7. Synthesis of [Pt{(TePPh$_2$)$_2$N}$_2$] [36] (**4**)

A solution of (TMEDA)Na[(TePPh$_2$)$_2$N] (0.80 g, 0.99 mmol) in THF (25 ml) was added via cannula to a solution of $PtCl_2$ (0.13 g, 0.50 mmol) in THF (15 ml) at room temperature. The solution turned brown immediately and was stirred for 2 h, followed by solvent removal under reduced pressure. Fresh THF (25 ml) was added and the solution filtered. The clear yellow filtrate was concentrated under vacuum and hexane (30 ml) was added. This was refrigerated, after which the solvent was removed to give a yellow powder. Yield: 0.30 g, 42%. Elemental analysis calculated for $C_{48}H_{40}PtN_2P_4Te_4$: C, 39.09; H, 2.74; N, 1.90; P, 8.41%. Found: C, 40.93; H, 3.45; N, 2.54; P, 9.85%. ^{1}H NMR (δ, ppm, $CDCl_3$, 400 MHz): 6.8–8.0 (m, Ar*H*); ^{31}P {^{1}H} NMR (δ, ppm, $CDCl_3$): 27.27.

2.8. Pyrolysis of the precursors

The pyrolysis experiments were carried out in a quartz glass tube reactor using a Carbolite heating furnace. Samples were heated at 500 °C under vacuum for 90 min and subsequently cooled to room temperature for 1 h under nitrogen. 500 mg of the sample was used for each experiment. Black deposits were obtained and pulverized afterwards, prior to subsequent characterisation methods.

2.9. Characterisation of the black deposits

X-ray diffraction studies were performed on a Bruker AXS D8 diffractometer using monochromated Cu-Kα radiation. The samples were mounted flat and scanned from 10 to 80° in a step size of 0.05 with a count rate of 9 s. The diffraction patterns were then compared to the documented patterns in the ICDD index. SEM was performed using a Philips XL30 FEG SEM. All deposits were coated with carbon to avoid charging of the sample by the electron beam, using Edward's coating system E306A before scanning electron microscopy (SEM) was carried out. Energy dispersive X-ray (EDX) analyses were done using a DX4 instrument. The XPS spectra were recorded using a Kratos Axis Ultra spectrometer, employing a monochromated Al Kα X-ray source and an analyser pass energy of 80 eV (wide scans) or 20 eV (narrow scans), resulting in a total energy resolution of *ca.* 1.2 and 0.6 eV, respectively. Uniform charge neutralisation of the photoemitting surface was achieved by exposing the surface to low energy electrons in a magnetic immersion lens system (Kratos Ltd). The system base pressure was 5×10^{-10} mBar. Spectra were analysed by first subtracting a Shirley background and then obtaining accurate peak positions by fitting peaks using a mixed Gaussian/Lorenzian (30/70) line shape. During fitting, spin orbit split components were constrained to have identical line widths, elemental spin orbit energy separations and theoretical spin orbital area ratios. Quantitative analysis was achieved using theoretical Scofield elemental sensitivities and recorded spectrometer transmission functions. All photoelectron binding energies (BE) were referenced to C1s adventitious contamination peaks set at 285 eV BE. The analyser was calibrated using elemental references; Au 4f$_{7/2}$ (83.98 eV BE), Ag3d$_{5/2}$ (368.26 eV BE) and Cu2p$_{3/2}$ (932.67 eV BE).

3. Results and discussion

The ligand [HN(PPh$_2$)$_2$] was prepared from (Me$_3$Si)$_2$NH and PPh$_2$Cl, which were commercially available. This amine is a reagent with limited isolation and characterization [37,38]. The compound was reacted with sodium hydride yielding the sodium amide [NaN(PPh$_2$)$_2$], as previously reported without detailed characterization [6]. Oxidation of the amide with elemental tellurium in the presence of *N,N,N′,N′*-tetramethylethylenediamine (TMEDA) produced the ditellurido ligand (TMEDA)Na[(TePPh$_2$)$_2$N] (Scheme 1). The complexes were prepared by the addition of the corresponding metal salt to a solution of ligand in THF at room temperature (Scheme 2). All the complexes were highly unstable in air, which may have contributed to the marginally higher than expected values for the microanalytical results.

Complexes **2**, **3** and **4** were characterised by NMR spectroscopy (^{1}H and ^{31}P {^{1}H} NMR in $CDCl_3$). The ^{1}H NMR spectrum for complex **2** displayed multiplets between δ 6.5 and 8.3 ppm for the aromatic protons. For complex **3**, the multiplets for the aromatic protons were seen between δ 6.8 and 7.9 ppm. In the spectrum of complex **4**, the aromatic protons were observed between δ 6.8 and 8.0 ppm. Also, for these complexes, other singlet peaks were shown for protons in different environments, which indicated coupling with other spin-active nuclei, e.g. Ar*H*-Ar*H* and Ar*H*-P. For the ^{31}P {^{1}H} NMR spectra, a singlet peak was observed for complex **2** at δ 10.29 ppm, while that of complex **3** occurred at δ 22.4 ppm. For complex **4**, the singlet peak was at δ 27.27 ppm. For **1**, no NMR studies were conducted due to its paramagnetic nature.

3.1. Thermogravimetric analysis

The physical properties of complexes **1**–**4**, probed by thermogravimetry analysis (TGA), showed a single-step decomposition with a rapid weight loss (Fig. S1 ESI). However, [Fe{(TePPh$_2$)$_2$N}$_3$] (**1**) was an exception to this, having two decomposition steps. Although its decomposition occurred in two steps, the observed residue value of 25% is close to the calculated value of 22% for a residue containing $FeTe_2$ and elemental tellurium. [Ni{(TePPh$_2$)$_2$N}$_2$] (**2**) decomposed between 280 and 370 °C with a final residue of about 20%, which is higher than the calculated value of 14% for NiTe from the precursor. The rapid weight loss of [Pd{(TePPh$_2$)$_2$N}$_2$] (**3**) occurred between 270 and 363 °C, with a residue amount of 20%, which is close to the 17% calculated value for PdTe in the precursor. The decomposition of [Pt{(TePPh$_2$)$_2$N}$_2$] (**4**) was between 274 and 348 °C, with 18% final residue, which is also almost in agreement with the calculated value of 22% for PtTe.

3.2. Pyrolysis of the complexes

Complex **1** was pyrolyzed at 500 °C and black deposits were obtained, pulverized and analysed by XRD. The sample formed

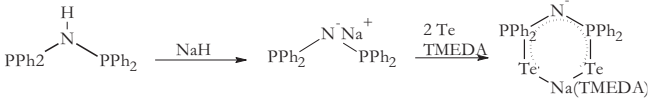

Scheme 1. Synthesis of the ditelluroimidodiphosphinate ligand.

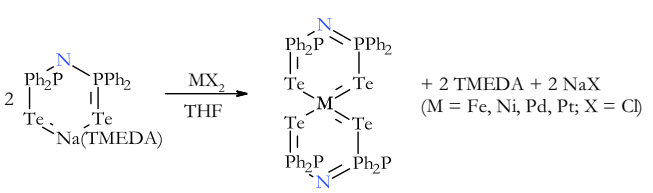

Scheme 2. Synthesis of the ditelluroimidodiphosphinate complexes.

was orthorhombic iron telluride $FeTe_2$ (ICDD 04-003-2015) and hexagonal tellurium (ICDD 01-079-0736) (Fig. 1a). Tellurium gave peaks from the primary reflections of 2-theta at 23.02°, corresponding to the (1 0 0) plane, and additional reflections of 2-theta at 27.56, 38.28, 43.35, 45.94 and 62.85° for the (0 1 1), (0 1 2), (1 1 1), (0 0 3) and (1 1 3) planes, respectively. The lattice parameter of $a = 5.290(8)$ Å is a close match with the literature value (Table S1, ESI). The deposited material consists of crisp flakes, as revealed by the SEM (Fig. 2a). EDX analysis showed the iron to tellurium ratio as 29.8:59.7% respectively, together with phosphorus contamination (*ca* 10%). The deposition of a metal telluride and tellurium might be expected since this had been previously reported [12,21]. It might be explained that the high ratio of Te:M in the precursor could be responsible for the deposition of elemental tellurium [1].

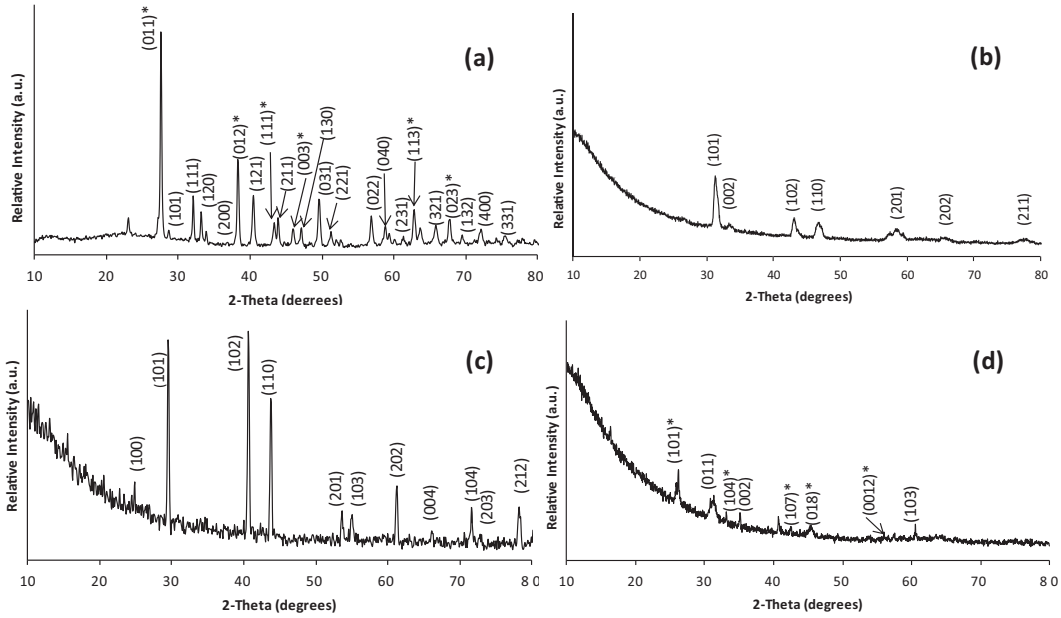

Fig. 1. XRD patterns of (a) orthorhombic $FeTe_2$ and hexagonal tellurium from **1**. * indicates tellurium, (b) hexagonal nickel telluride from **2**, (c) hexagonal palladium telluride deposited from **3** and (d) hexagonal $PtTe_2$ and rhombohedral PtTe from **4**. All depositions were at 500 °C.

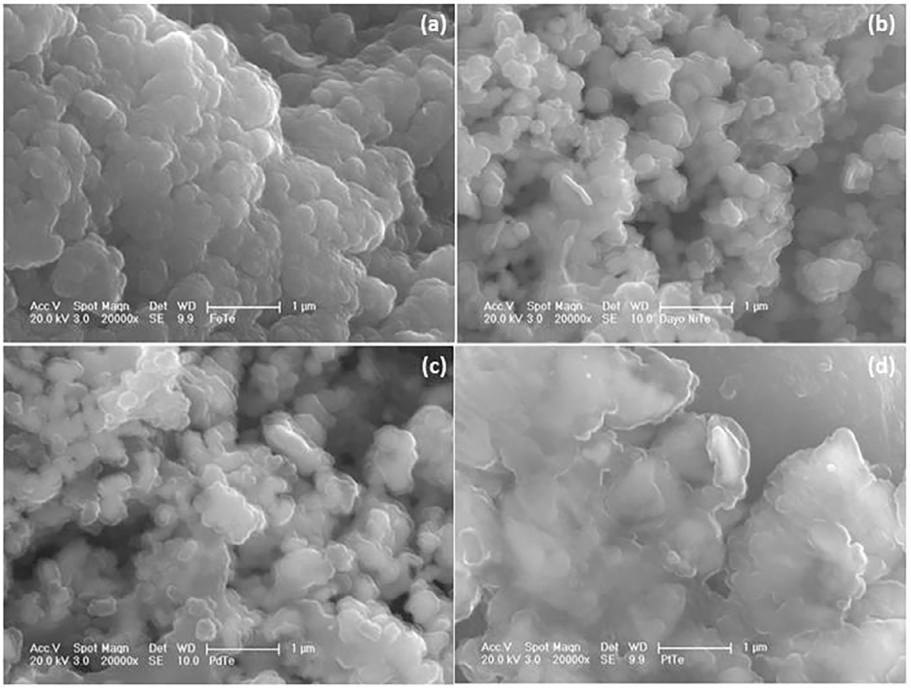

Fig. 2. SEM images of: (a) iron telluride and tellurium from **1**, (b) nickel telluride from **2**, (c) palladium telluride from **3** and (d) platinum telluride from **4**. All depositions occurred at 500 °C. Scale size = 1 µm.

Complex **2** was pyrolysed at 500 °C under a constant flow of nitrogen, which gave a black deposit that was later pulverized prior to XRD analysis. XRD of the pyrolysed sample confirmed the deposition of hexagonal nickel telluride NiTe (ICDD 00-038-1393), having the preferred orientation along the (1 0 1) plane (Fig. 1b). SEM studies to determine the morphology of the material revealed them to be tiny fused crystallites of nickel telluride (Fig. 2b). The obtained lattice parameters of $a = 3.930(3)$ Å, and $c = 5.367(4)$ Å are in agreement with reported values in the literature (Table S1, ESI). EDX analysis on the hexagonal crystallites showed a high nickel content, with nickel and tellurium having 43.9 and 26.3%, respectively, together with phosphorus contamination (29.8%). In a previous study, hexagonal nickel telluride $Ni_{0.51}Te$ was also deposited from $[Ni\{(SeP^iPr_2)(TeP^iPr_2)N\}_2]$ [21a].

The pyrolysis of complex **3** at 500 °C also produced a black residue, which was analysed by XRD. The sample formed was hexagonal palladium telluride PdTe (ICDD 00-029-0971) (Fig. 1c). The obtained lattice parameters match closely with the reported values, $a = 4.132$ Å (Table S1, ESI). The deposited material consists of globular crystallites of palladium telluride, as indicated by SEM (Fig. 2c). EDX analysis on the sample revealed a high tellurium content with a Pd:Te ratio of 30.1:56.8% respectively, together with phosphorus (13.2%).

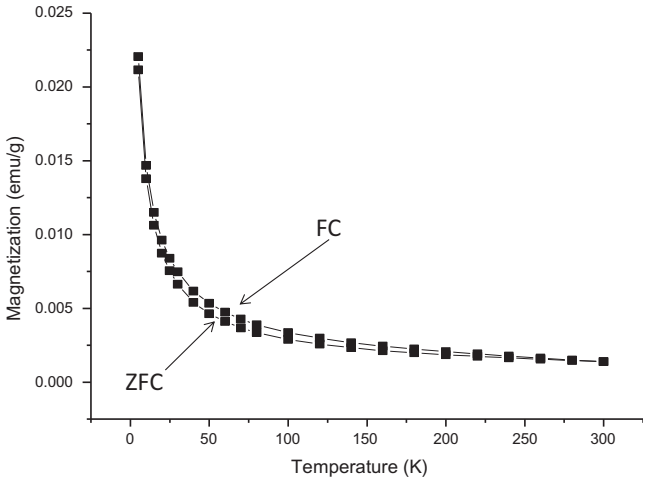

Fig. 3. Zero field-cooled (ZFC) and field-cooled (FC) curves of hexagonal iron telluride deposited from $[Fe\{(TePPh_2)_2N\}_3]$ (**1**) at 100 0e.

The pyrolysis of complex **4** at 500 °C also deposited a black residue, which was analysed by XRD. The X-ray diffraction pattern revealed a mixture of both rhombohedral platinum telluride PtTe (ICDD 01-088-2262) and hexagonal platinum telluride $PtTe_2$ (ICDD 04-003-1897) (Fig. 1d). Traces of PtTe were observed at 2-theta values of 26.32, 31.60, 41.10, 44.84, 55.11 and 56.66°. These correspond to the (1 0 1), (1 0 4), (1 0 7), (0 1 8), (0 0 1 2) and (0 2 4) planes, respectively. The lattice parameters indicated values of 4.027 and 5.223 Å for *a* and *c*, respectively. SEM analysis of the deposited powder showed the morphology to be uniformly arranged flat flakes of platinum telluride (Fig. 2d). EDX analysis on the deposited sample indicated the values for platinum and tellurium to be 32.8 and 40.3% respectively, with phosphorus as 26.9%.

3.3. Magnetic measurements and XPS analysis on iron telluride

Iron tellurides are antiferromagnetic materials whose magnetic properties depend on the temperature between 2.5 and 300 K [28,41,42]. From the magnetic measurements, it should be possible to evaluate phase relationships which exist in iron telluride systems.

DC magnetization plots of $FeTe_2$ powders deposited from $[Fe\{(TePPh_2)_2N\}_3]$ (**1**) are shown in Fig. 3. Magnetization versus temperature for ZFC and FC experiments at 100 Oe magnetic fields are given in Fig. 3, which shows the superimposition of the ZFC and FC curves on each other and their values increased with decreasing temperature. Hence, this might indicate the antiferromagnetic behaviour of the sample.

In the amorphous state, $FeTe_2$ displays a strong antiferromagnetic coupling between localized moments, though without a long-range magnetic ordering, and transits to a spin-glass state at 6 K [28,43]. However, the crystalline state shows 3D antiferromagnetic ordering at ~83 K [44]. From Fig. 3 shown above, we can assume that the antiferromagnetic transition temperature, T_N, occurs at around 75 K. Previously, the magnetic properties of various iron and tellurium having integral stoichiometric ratios have been studied. An example is FeTe as an antiferromagnetic material with a transition temperature of 70 K [45], while $FeTe_2$ transits as an antiferromagnetic material at 100 K [28].

The surface atomic coverage and surface chemistry of the powder obtained from **1** were determined by XPS. The Fe 2p peak appeared at 714 and 728 eV for $2p_{3/2}$ and $2p_{1/2}$, respectively (Fig. S2, ESI). This indicates iron oxide/hydroxide, suggesting the probable surface oxidation of the sample prior to XPS analysis. Iron

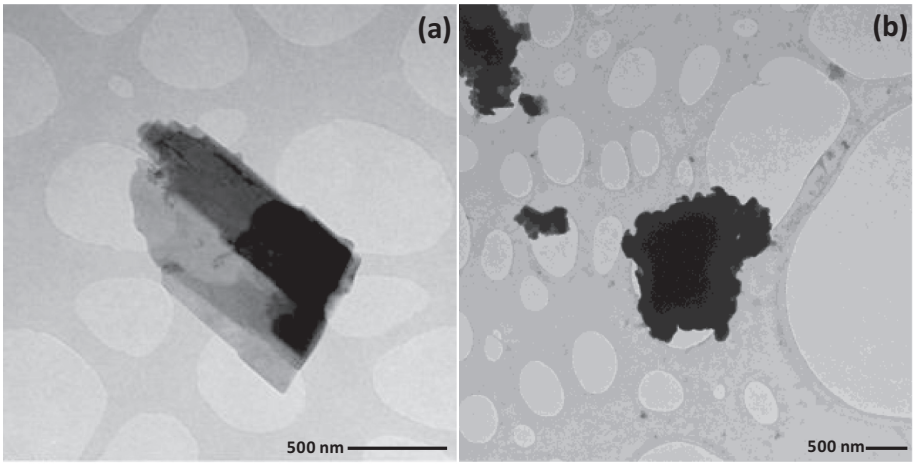

Fig. 4. TEM images of (a) palladium telluride and (b) nickel telluride.

telluride should have a binding energy at 707 eV for the $2p_{3/2}$ peak [39]. Furthermore, the tellurium 3d scan showed a weak peak at *ca.* 576 eV, which only matches tellurium oxide species (Fig. S3, ESI). Typically, tellurium 3d has binding energies at 572–573 eV [40]. It is possible that this sample might have been oxidised in the course of other analyses (e.g. SEM, XRD).

3.4. Conductivity studies on NiTe and PdTe

Films of each of the samples were prepared by vacuum-filtering their dispersion onto a PVDF membrane. The film was dried at 60 °C under vacuum for 24 h. Four silver electrodes were then painted onto the surface of the film and four silver wires were attached to the electrodes. After connecting the wires to a Keithley source meter, I-V curves showed no current, implying a high resistance. The TEM images of the prepared flakes of the samples revealed their 2D structures, as shown in Fig. 4.

4. Conclusions

Ditelluridoimidodiphosphinate complexes $[M\{(TePPh_2)_2N\}_2]$ (M = Ni, Pd, Pt) and the iron (III) complex $[Fe\{(TePPh_2)_2N\}_3]$ have been synthesised from $Na^+[N(PPh_2)_2]^-$ after its reaction with elemental tellurium. The thermal properties of the complexes were suitable for the synthesis of metal tellurides. Scanning electron microscope images of the powders showed predominantly polygonal crystallites, ranging from crisp flakes of $FeTe_2$ to globular crystallites of PtTe. Conductivity studies on NiTe and PdTe showed these materials to be insulating. Future work on these tellurium complexes will involve the preparation of the isopropyl analogues and investigations of their potential for passivated nanocrystals through colloidal routes.

Conflicts of interest

There are no conflicts to declare.

Acknowledgements

T.O. acknowledges the School of Chemistry, the University of Manchester for funding. The authors will like to thank Prof. Jonathan Coleman for assistance on the conductivity studies of some samples. We are grateful to Dr. Paul Wincott and Dr. Floriana Tuna for XPS and SQUID measurements, respectively.

Appendix A. Supplementary data

Supplementary data to this article can be found online at https://doi.org/10.1016/j.poly.2018.12.038.

References

[1] T. Chivers, J.S. Ritch, S.D. Robertson, J. Konu, H.M. Tuononen, Acc. Chem. Res. 43 (2010) 1053.
[2] T. Chivers, M. Parvez, G.G. Briand, Angew. Chem. Int. Ed. 41 (2002) 3468.
[3] S.B. Trivedi, C.-C. Wang, S. Kutcher, U. Hommerich, W. Palosz, J. Cryst. Growth 310 (2008) 1099.
[4] L.M. Goncalves, C. Couto, P. Alpuim, J.H. Correia, J. Micromech. Microeng. 18 (2008) 064008.
[5] T. Chivers, D.J. Eisler, J.S. Ritch, Dalton Trans. (2005) 2675.
[6] J.S. Ritch, T. Chivers, D.J. Eisler, H.M. Tuononen, Chem.-Eur. J. 13 (2007) 4643.
[7] (a) V.B. Anzin, Y.V. Kosichkin, A.I. Nadezhdinskii, Phys. Status Solidi A 20 (1973) 253;
(b) Z.H. Wang, L.L. Wang, J.R. Huang, J. Mater. Chem. 20 (2010) 2457.
[8] (a) D. Royer, E. Dieulesaint, J. Appl. Phys. 50 (1979) 4042;
(b) D.V. Damodara, N. Jayaprakash, N. Soundararajan, J. Mater. Sci. 16 (1981) 3331.
[9] Y. Wang, Z. Tang, P. Podsiadlo, Adv. Mater. 18 (2006) 518.
[10] S.S. Garje, J.S. Ritch, D.J. Eisler, M. Afzaal, P. O'Brien, T. Chivers, J. Mater. Chem. 16 (2006) 966.
[11] J.S. Ritch, T. Chivers, K. Ahmad, M. Afzaal, P. O'Brien, Inorg. Chem. 49 (2010) 1198.
[12] S.S. Garje, M.C. Copsey, M. Afzaal, P. O'Brien, T. Chivers, J. Mater. Chem. 16 (2006) 4542.
[13] Y.P. Yadava, R.A. Singh, J. Mater. Sci. Lett. 4 (1985) 1421.
[14] W. Klemm, N. Frantini, Z. Anorg. Allgem. Chem. 251 (1943) 222.
[15] E.F. Westrum, C. Chou, R.E. Machol, F. Gronvold, J. Chem. Phys. 28 (1958) 497.
[16] (a) S.A. Shchukarer, M.S. Apurina, Russ. J. Inorg. Chem. 5 (1960) 1167;
(b) Q. Peng, Y. Dong, Y. Li, Inorg. Chem. 42 (2003) 2174.
[17] M. Ettenberg, K.L. Komarek, E. Miller, J. Solid State Chem. 1 (1970) 583.
[18] I. Oftedal, Z. Phys. Chem. 128 (1927) 135.
[19] S. Tengnér, Z. Anorg. Allgem. Chem. 239 (1938) 126.
[20] A.K. Dua, R.P. Agarwala, Thin Solid Films 8 (1971) 307.
[21] (a) S.D. Robertson, T. Chivers, J. Akhtar, M. Afzaal, P. O'Brien, Dalton Trans. (2008) 7004;
(b) Y. Mu, Q. Li, P. Lv, Y. Chen, D. Ding, S. Su, L. Zhou, W. Fu, H. Yang, RSC Adv. 4 (2014) 54713.
[22] L. Thomassen, Z. Phys. Chem. 4B (1929) 277.
[23] L. Wöhler, K. Ewald, H.G. Krall, Ber. Deu. Chem. Ges. 66 (part IIB) (1933) 1638.
[24] W.O.J. Groeneveld Meijer, Am. Min. 40 (1955) 646.
[25] A. Vymazalová, P. Ondrus, M. Drábek, Min. Dep. Res., Meeting the global Challenge, session 13 (2005) 1439.
[26] (a) H.-H. Li, S. Zhao, M. Gong, C.-H. Cui, D. He, H.-W. Liang, L. Wu, S.-H. Yu, Angew. Chem. Int. Ed. 52 (2013) 1;
(b) A.B. Karki, D.A. Browne, S. Stadler, J. Li, R. Jin, J. Phys.: Condens. Matter 24 (2012) 055701.
[27] F. Grønvold, H. Haraldsen, A. Kjekshus, Acta Chem. Scand. 14 (1960) 1879.
[28] J.H. Zang, B. Wu, C.J. O'Connor, W.B. Simmons, J. Appl. Phys. 73 (1993) 5718.
[29] L.D. Dudkin, V.I. Vaidanich, Sov. Phys. Solid State 2 (1961) 138.
[30] L.D. Dudkin, V.I. Vaidanich, Sov. Phys. Solid State 6 (1962) 1384.
[31] W. Zhang, Z. Yang, J. Zhan, L. Yang, W. Yu, G. Zhou, Y. Qian, Matt. Lett. 47 (2001) 367.
[32] M. Bochmann, Chem. Vap. Dep. 2 (1996) 85.
[33] M.L. Steigerwald, Chem. Mater. 1 (1989) 52.
[34] X.J. Song, M. Bochmann, J. Chem. Soc., Dalton Trans. (1997) 2689.
[35] N. Levesanos, S.D. Robertson, D. Maganas, C.P. Raptopoulou, A. Terzis, P. Kyritsis, T. Chivers, Inorg. Chem. 47 (2008) 2949.
[36] S.D. Robertson, J.S. Ritch, T. Chivers, Dalton Trans. (2009) 8582.
[37] D. Cupertino, D.J. Birdsall, A.M.Z. Slawin, J.D. Woollins, Inorg. Chim. Acta 290 (1999) 1.
[38] A.M.Z. Slawin, J. Ward, D.J. Williams, J.D. Woollins, J. Chem. Soc. Chem. Commun. (1994) 421.
[39] D. Telesca, Y. Nie, J. I. Budwick, B. O. Wells, B. Sinkovic, cond-mat.supr-con., (2011) arXiv:1102.2155.
[40] S. Jobic, R. Brec, J. Rouxel, J. Solid St. Chem. 96 (1992) 169.
[41] A.A. Temperly, H.W. Lefevre, J. Phys. Chem. Solids 27 (1966) 85.
[42] S. Chiba, J. Phys. Soc. Japan 10 (1955) 837.
[43] W. Zhang, Y. Cheng, J. Zhan, W. Yu, L. Yang, L. Chen, Y. Qian, Matt. Sci. Engnr B 79 (2001) 244.
[44] J.P. Llewellyn, T. Smith, Proc. Phys. Soc. 74 (1959).
[45] D.E. Gray (Ed.), American Institute of Physics Handbook, 2nd ed., McGraw-Hill, New York, 1963, pp. 5–200.